Source and receiver ghost effects in seismic illumination using wave equation

Luana Nobre Osorio[1], André Bulcão[2], Bruno Pereira-Dias[2], Josias J. Silva[3], Luiz Landau[1]
[1] COPPE – Federal University of Rio de Janeiro
[2] CENPES/PETROBRAS
[3] PETREC – Petroleum Research and Technology

This paper was prepared for presentation during the 14th International Congress of the Brazilian Geophysical Society held in Rio de Janeiro, Brazil, August 3-6, 2015.

Abstract

This paper presents a study of seismic illumination using a wave-equation-based method. The objective is to evaluate seismic marine acquisition parameters taking into account source and receiver ghost effects. Numerical results of homogeneous medium and a modified Hess model are presented and analyzed.

Introduction

In the recent years there has been a great interest in preserving a broadband spectrum of seismic data (see e.g. Cunha Filho, 2014). The source and receiver ghosts are a main reason for the limitation of the seismic spectrum, causing an uneven response in the low and high frequency information of the seismic data. This degradation of the seismic signal can be harmful for the convergence of several seismic inversion algorithms.

Along with phase modification caused by the ghosts, the seismic amplitude is also modified. This has a direct effect for the seismic illumination. Illumination studies should also take into account geological complexity and acquisition geometry. The lack of homogeneous illumination causes a distorted image.

In order to evaluate the effect of the acquisition geometry in marine data, illumination is calculated and data is modeled with source and/or receiver ghost. It is also analyzed the frequency content considering both configurations.

Method

For a seismic marine acquisition, the free surface is considered to have a negative reflection coefficient. As can be seen from Figure 1, for both ghosts the polarity is reverse. Figure 1 shows a typical receiver and source ghost generation, the two ghosts have reverse polarity related to the primary event. The sum of the primary and the ghost event has a direct effect on the amplitude and phase spectra of the seismic signal. The ghost response can be estimated by (Rosa, 2010):

$$A_G(\omega) = \left| 2\sin\left(\frac{\omega\tau}{2}\right) \right|, \quad (1)$$

$$\phi_G(\omega) = \frac{\omega\tau}{2} - \frac{\pi}{2}, \quad (2)$$

where A_G and ϕ_G are respectively the amplitude and phase spectra; τ is the ghost delay.

The notch is created in multiples of frequency:

$$f = \frac{1}{\tau} = \frac{v}{2d\cos\theta}, \quad (3)$$

where d is the source or receiver depth and v is the propagation velocity in the media. θ is the incidence (receiver) or departure (source) angle.

Equation (1) puts in evidence that the ghost effect can have a doubling energy effect when $\omega\tau = 2n\pi$ (n=0,1,2...), or a notch effect when $\omega\tau = 2\pi(n + 1/2)$ (n=0,1,2...). This clearly affects the seismic energy and cannot be neglected in illumination studies.

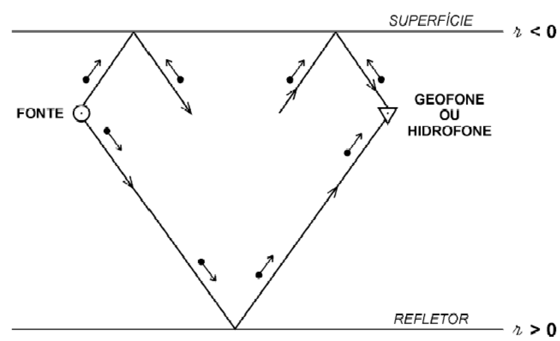

Figure 1 Typical generation of receiver and source ghosts (Figure extracted from *Rosa*, 2010*)*

Seismic Illumination Studies can be understood as the effort involved in determining which regions have high amplitudes and can present shadow zones of propagated wavefields, considering a specific acquisition planning (Laurain et al., 2004). The Illumination Energy is defined in this case as the energy of the wavefield propagated for a simulation time at each point of the velocity model.

The proposed methodology is based on solutions for the Acoustic Wave Equation obtained by FDM (Finite

Difference Method). The first step involves a wavefield extrapolation from the target up to the surface, applying the Reciprocity Principle like Alves et al. (2008).

According to Alves *et al.* (2009), the illumination energy is given by the sum of the energy source times the integral over the receiver surface for a specific source Ω_s, expressed as:

$$I(\vec{r}) \cong \sum^{Sources} E_D(\vec{r},\vec{r}_s).\int E_U(\vec{r},\vec{r}_R)\,d\Omega_s \qquad (4)$$

where: I is illumination energy at the investigated point $\vec{r}$; $\vec{r}_s$ and $\vec{r}_R$ are the source and the receiver locations; E_D and E_U are, respectively, the downgoing and upgoing energy matrices of wavefields and Ω_s is formed by the receiver area considering a specific source location.

Numerical Examples

This methodology was applied firstly to a homogenous model and the modified Hess Model[1]. Figures 3 and 8 show the velocity models with the illumination point. In Figure 8, the chosen illumination point was underneath the high velocity body.

A broadband Butterworth wavelet (2-40 Hz) with was used as source for the synthetic examples (shown in Figure 2). Using this source type it is possible to have a large frequency bandwidth and better evaluate the ghost effects.

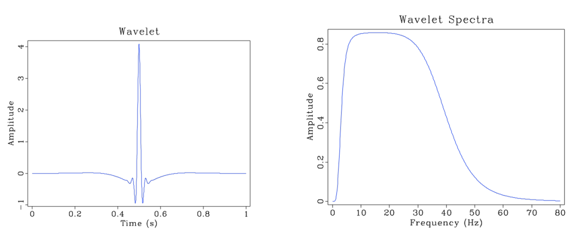

Figure 2: Source wavelet used (left) and its frequency spectrum (right).

The energy vector can be obtained by calculating the energy over the receiver position (as described in the previous section). For the selected point the energy vector was obtained over the entire velocity model for data modeling with and without ghost effects.

The comparison between the seismograms with and without the ghost is shown in Figure 4. Figure 5 shows the energy vector curve for data with and without ghost for a homogeneous model. It is possible that for the short offset there is an increased energy for the experiment with ghost. This is related to the doubling of event energy due to the ghost response. On the other side, for the long offsets, there is the cancellation of the primary and ghost energies that lead to a reduction of the energy in such region. The loss of low frequency energy is shown in Figure 6, and it is put in evidence that this effect has a greater influence on the long offset on Figure 7, which shows the frequency spectrum for each trace.

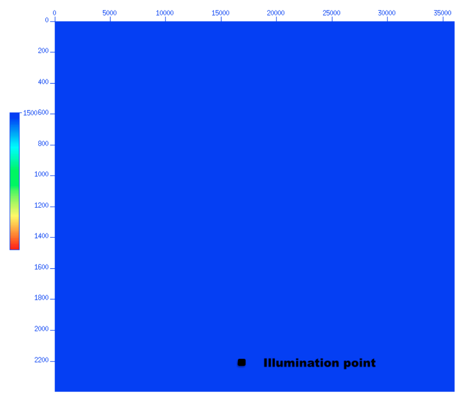

Figure 3: Homogeneous model with the illumination point.

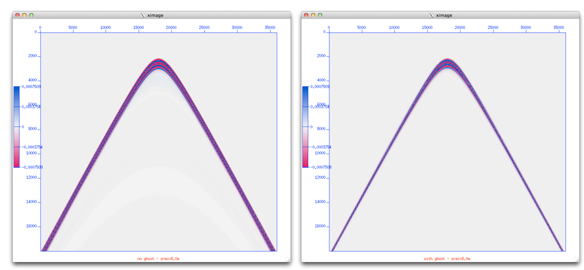

Figure 4: Seismogram without ghost (left) and with ghost (right) for homogeneous model.

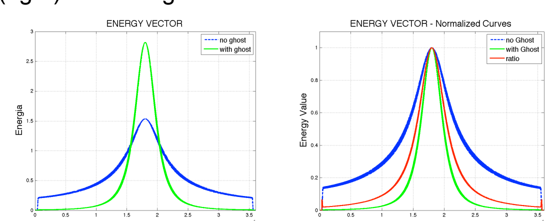

Figure 5: Energy vector (left) and normalized energy vector (right) for the homogeneous model with depth cable 8m.

[1] Hess VTI model was generated at Hess Corporation and released at http://software.seg.org/

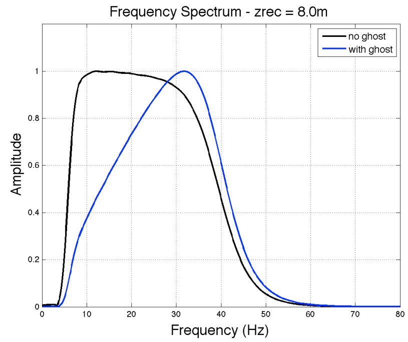

Figure 6: Average frequency spectrum for the homogeneous model

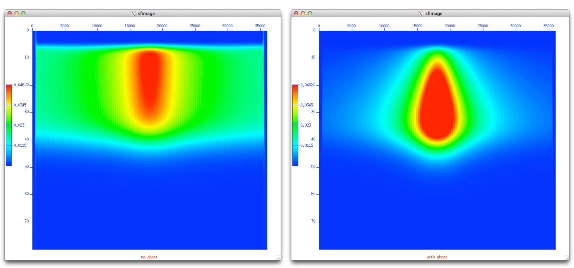

Figure 7: Frequency spectrum of each trace for the seismogram without ghost (left) and with ghost (right) for homogeneous model.

The second numerical experiment is realized on the Hess model (Figure 8). It was chosen two illumination points localized at the positions (x_1=13000m; z_1=8400m) and (x_2=13000m; z_2=2200m) from now on referred as illumination points 1 and 2, respectively.

It should be pointed out, that for the illumination study in this model, not only the ghost effect takes place but also geological complexity affects the results. The comparison of the frequency content and illumination energy for the point 1 and 2 are shown in the Figures 9-12 and 13-16, respectively.

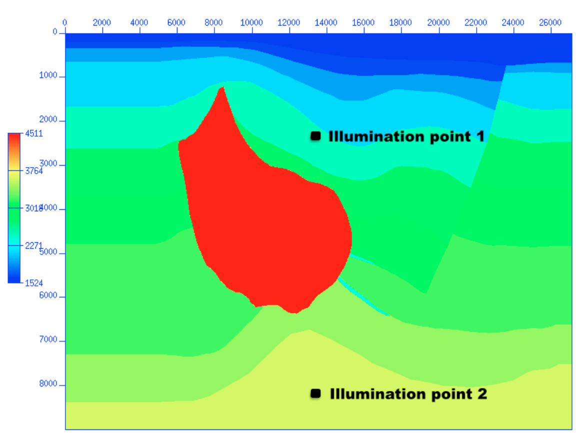

Figure 8: Illumination points for the Hess model

Conclusion and discussion

By the presented results we conclude that the ghost effects are relevant not only to the frequency bandwidth of the seismic data, but it also affects the seismic illumination, as shown in the homogeneous and Hess model. For short offsets (actually, low incidence or departure angles), the ghost signal shows an increase in the energy. On the other hand, long offsets (high incidence or departure angles) have a cancelling effect that can lower the seismic energy on the illumination point.

The increase of the energy illumination due to the ghost effect can be put for benefit for the final seismic image with dual sensor separation (Carlson et al. 2007) and mirror migration techniques (Soubaras, 2010). As for the energy cancellation of the long offsets, this should be taken into account for acquisition design with very long offset, due to the elevated financial cost of this type of acquisitions.

In further study of this work it will be considered the ghost effect for different cable depth and cable geometries, such as slanted cables (Soubaras and Dowle, 2010).

Acknowledgments

The authors from Federal University of Rio de Janeiro acknowledge the financial support of ANP and PETROBRAS for authorizing this publication.

References

Alves, G. C., A. Bulcão, D. M. Soares Filho, C. E. Theodoro, L. Santos, and M. Guimarães, 2008, Target-oriented illumination analysis using wave equation: 78th Annual International Meeting, SEG, Expanded Abstracts, 163–167.

Alves, G. C., A. Bulcão, D. M. Soares Filho, C. E. Theodoro, and L. A. Santos, 2009, Target-oriented-approach for illumination analysis using wave equation via FDM: 79th Annual International Meeting, SEG, Expanded Abstracts, 181–185.

Carlson, D.H.; Long, A.; Söllner; W.; Tabti, H.; Tenghamn, R. and Lundel, N., 2007 Increased resolution and penetration from a towed dual-sensor streamer: First Break, 25(12),71-77

Carlson, D.H.; Long, A.; Söllner; W.; Tabti, H.; Tenghamn, R. and Lundel, N., 2007 Increased resolution and penetration from a towed dual-sensor streamer: First Break, 25(12),71-77

Cunha Filho, C.A., 2014, Second EAGE/SBGf Workshop on Broadband Seismic 2014, 4-5 November 2014, Rio de Janeiro, Brazil

Laurain, R., L. Gelius, V. Vinje, and I. Lecomte, 2004, A review of 3D illumination studies: Journal of Seismic Exploration, 13, 17–37.

Rosa, A.L.R., 2010, Análise do sinal sísmico: Sociedade Brasileira de Geofísica.

Soubaras, R., and R. Dowle, 2010,Variable depth streamer—A broadband marine solution: First Break, 28, 89-96

Soubaras, R., 2010, Deghosting by joint deconvolution of a migration and a mirror migration: 80th Annual International Meeting, SEG, Expanded Abstracts, 3406-3410.

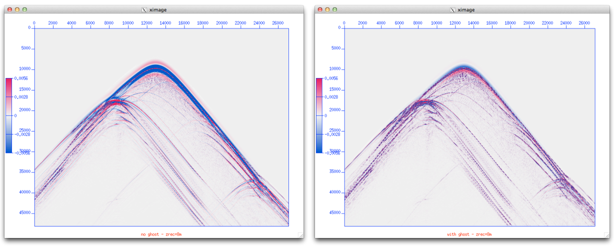

Figure 9: Seismogram without ghost (left) and with ghost (right) for Hess model (illumination point 1).

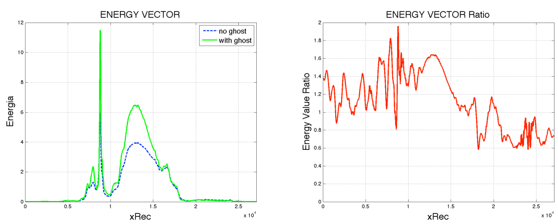

Figure 10: Energy vector (left) and energy vector Ratio (right) for the Hess model (illumination point 1) with depth cable 8m.

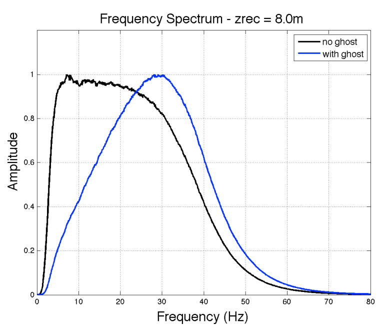

Figure 11: Average frequency spectrum for the Hess model (illumination point 1)

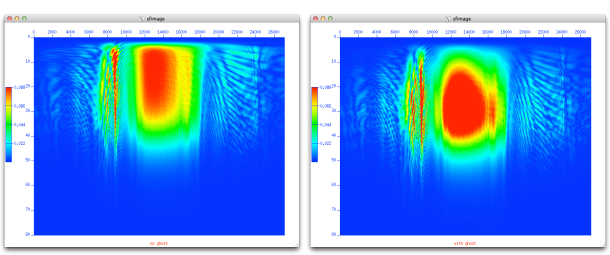

Figure 12: Frequency spectrum of each trace for the seismogram without ghost (left) and data with ghost (right) for Hess model (illumination point 1).

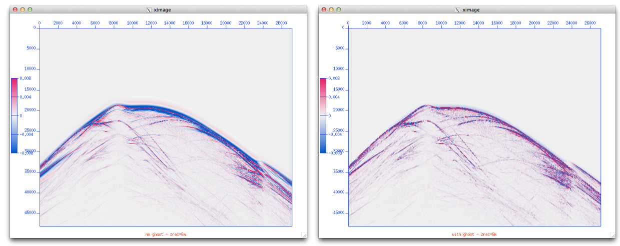

Figure 13: Seismogram without ghost (left) and with ghost (right) for Hess model (illumination point 2).

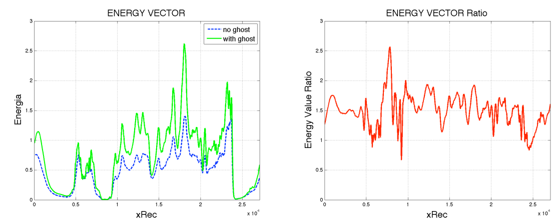

Figure 14: Energy vector (left) and energy vector Ratio (right) for the Hess model (illumination point 2) with depth cable 8m.

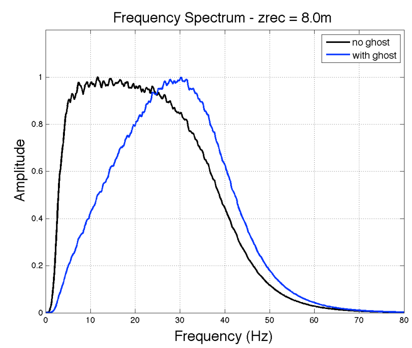

Figure 15: Average frequency spectrum for the Hess model (illumination point 2)

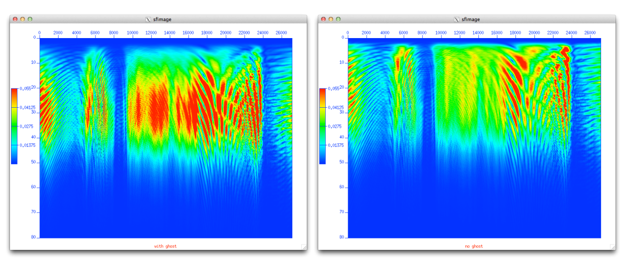

Figure 16: Frequency spectrum of each trace for the seismogram without ghost (left) and data with ghost (right) for Hess model (illumination point 2).